

# Charge Transfer from Adsorbed Proteins

K. Bradley,<sup>\*†</sup> M. Briman,<sup>‡</sup> A. Star,<sup>†</sup> and G. Grüner<sup>†,‡</sup>

*Nanomix Inc., Emeryville, California 94608, and Department of Physics and Astronomy, University of California at Los Angeles*

*Received November 5, 2003; Revised Manuscript Received December 16, 2003*

## ABSTRACT

We have used transistor devices with carbon nanotubes as the conducting channel to explore the interaction between the nanotube surface and streptavidin, both in dry and in buffer environments. We find charge transfer between the protein and the nanotubes in both cases. Comparison with simpler molecules allows the estimation of the transferred charge. We argue that this effect can be understood as being due to the interaction between the  $-\text{NH}_2$  groups of the protein and the aromatic surface.

Because of the rich potential of nanobiotechnology, including biosensors<sup>1</sup> and bioelectronics,<sup>2</sup> recent research has focused on the interactions between biomolecules and inorganic systems. A major goal continues to be the fabrication of structures of proteins immobilized on various functional surfaces while preserving the biological activity of the proteins.<sup>3,4</sup> A variety of mechanisms have been explored for immobilization, including covalent bonding,<sup>5</sup> hydrophobic interactions, and charge-transfer-induced adsorption.<sup>6</sup> The most direct evidence has been provided by scanning force microscopy, which in recent years has been used to measure the strength of protein attachment.<sup>7</sup> Here we use a semiconducting substrate, a carbon nanotube, to demonstrate directly the importance of charge transfer in the adsorption of streptavidin.

Carbon nanotubes are important elements at the intersection of biotechnology and materials science. Nanotubes have been functionalized to be biocompatible and to be capable of recognizing proteins.<sup>8–11</sup> Often, this functionalization has involved noncovalent binding between a bifunctional molecule and a nanotube to anchor a bioreceptor molecule with a high degree of control and specificity. The unique geometry of nanotubes has also been used to modify nanotube–protein binding. The conformational compatibility, driven by both steric and hydrophobic effects, between proteins and carbon nanotubes has been examined using streptavidin and other proteins. For example, streptavidin has been crystallized in a helical conformation around multiwalled carbon nanotubes.<sup>12</sup> Conversely, the tendency of biological materials to self-organize has been used to direct the assembly of nanotube structures.<sup>13</sup>

We have explored the details of the nanotube–protein interaction by using a nanoscale electronic device in which a single-walled carbon nanotube acts as the semiconducting channel of a field-effect transistor. Such devices have been extensively studied<sup>14</sup> since first being fabricated in 1998.<sup>15</sup> In our device, the ability to measure the electronic properties of the nanotube allows us to query the electronic state of the immobilization substrate. This ability makes such devices promising candidates for the electronic detection of biological species,<sup>16</sup> and they have demonstrated the potential for specific protein recognition.<sup>17,18</sup>

The experimental configuration includes a nanotube transistor, as depicted in Figure 1, fabricated using CVD growth and Ti/Au contacts.<sup>19</sup> Two types of measurement of the device transfer characteristics were performed. In the first, the current through the drain contact (at fixed source-drain bias) was monitored while a variable gate voltage (4 Hz, 20  $V_{\text{pp}}$ ) was applied to a metallic gate buried underneath the  $\text{SiO}_2$  substrate. This measurement is referred to as a substrate–gate transfer characteristic. In the second, the device was immersed in a buffer solution. A variable gate voltage (0.5 Hz, 1  $V_{\text{pp}}$ ) was applied through a platinum electrode. The current through the drain contact was recorded simultaneously with the voltage between the drain contact and a silver reference electrode in the solution. During these measurements, the apparatus was shaken gently using a lab rotator at 3 Hz. These measurements are referred to as liquid–gate transfer characteristics.<sup>20,21</sup>

The effect of protein adsorption was studied with both measurements. Devices were incubated with streptavidin at 40 nM in a 15 mM phosphate buffer at 25 °C. Liquid–gate transfer characteristics were measured continually during the incubations. After 10 h, the devices were rinsed with distilled

\* Corresponding author. E-mail: kbradley@nano.com.

† Nanomix Inc.

‡ University of California at Los Angeles.



**Figure 1.** AFM image of a nanotube device after a brief incubation with protein. Individual proteins and clumps of proteins are observed to be adsorbed both to the silicon oxide substrate and to the nanotube.

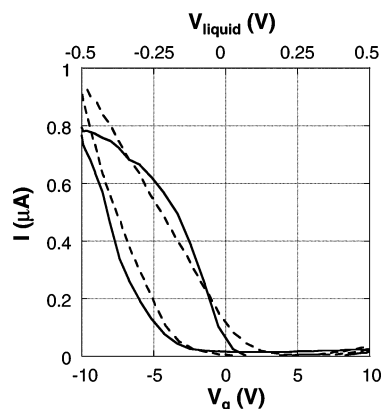
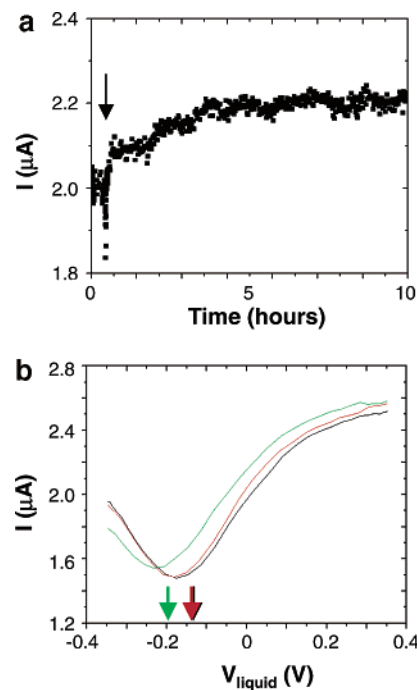


**Figure 2.** NT-FET transfer characteristics in air (solid line), using the bottom gate, and in water (dotted line), using the liquid gate. Note the different x scales for the bottom gate and the liquid gate.

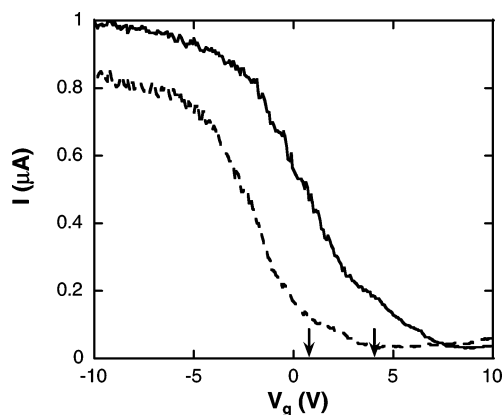
water and blown dry, and the substrate-gated transfer characteristics of the dried devices were measured.

Figure 2 compares the resulting transfer characteristics in the absence of biological molecules. The devices are field-effect transistors, with p-type conduction at negative gate voltages. In some devices, n-type conduction was also observed at positive gate voltages. The substrate-gate and liquid-gate characteristics are different because the capacitance between the nanotube and the two gates is different. However, when the curves are scaled by a factor of 20, they overlap, as Figure 2 indicates. This observation has previously been used to estimate the amount of charge donated by ammonia molecules on nanotubes.<sup>22</sup>

During the incubation with protein, the device electronic properties changed over time, as Figure 3 illustrates. The device was measured using the liquid-gated configuration, and Figure 3A shows the time dependence of the current at 20 mV. Immediately after the introduction of protein into the buffer solution, the device current began to increase



**Figure 3.** (a) Current versus time for a nanotube device incubated with 40 nM streptavidin.  $V_g = 20$  mV, and  $V_{sd} = 10$  mV. The arrow indicates the addition of streptavidin. (b) Current versus gate voltage (liquid gate) for the nanotube device.  $V_{sd} = 10$  mV. Red, in phosphate buffer before streptavidin addition. Black, same conditions, to measure the uncertainty in the threshold voltage. Green, after 10 h of incubation with streptavidin. Arrows indicate the threshold voltages for the three curves.



**Figure 4.** Current versus gate voltage (substrate) for a nanotube device in air. ( $V_{sd} = 0.4$  V) Solid line, before protein exposure. Dashed line, after 30 min of incubation with 2.5  $\mu$ M streptavidin. Arrows indicate the threshold voltages for the two curves.

gradually; it continued to increase over several hours of incubation. This change in current results from a rigid shift of the full liquid-gated transfer characteristic, as shown in Figure 3B. The magnitude of the shift at the end of incubation could be clearly distinguished from the random shifts due to fluctuations in the buffer (temperature, pH, etc.), indicated by the red and black curves in Figure 3B. After drying, the substrate-gated transfer characteristics (Figure 4) were similarly shifted with respect to the curves measured before incubation.

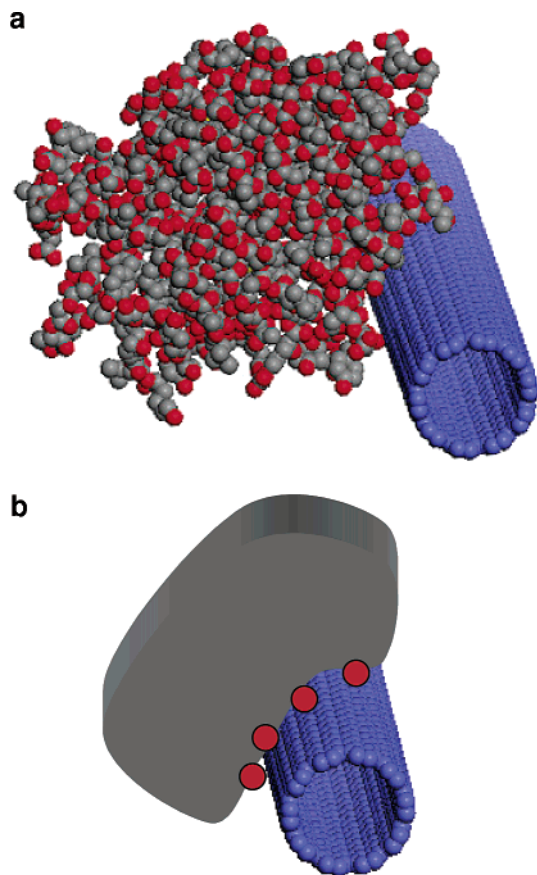


**Figure 5.** (a) Size comparison between a carbon nanotube and a streptavidin molecule. In the protein model, nitrogen atoms are red. (b) Schematic of nanotube–protein interaction. The protein is modeled as a deformable blob that contacts the nanotube with amine groups, indicated by red dots.

We will discuss these results in terms of a simple model in which adsorbed streptavidin coats the single-walled nanotube. The gradual shift in the threshold voltage is assumed to result from the slow accumulation of a full monolayer of adsorbed protein. This coverage-dependent threshold shift is analogous to the concentration-dependent shift observed when such devices are exposed to aqueous ammonia.<sup>22</sup> In the case of ammonia, the shift can be correlated to the concentration because the highly mobile adsorbate layer equilibrates quickly. By contrast, the protein adsorbate equilibrates over several hours so that only the full monolayer can be conclusively determined.

Such protein monolayers have previously been observed to form under a variety of conditions, especially at interfaces, which permit protein crystallization. Proteins have also been crystallized on the sidewalls of multiwalled carbon nanotubes; nanotube-supported streptavidin crystals have helical character and a thickness of 5 nm.<sup>12</sup> This thickness is consistent with the size of a streptavidin molecule and demonstrates that a single protein layer coated those nanotubes. The similarity of streptavidin organization on nanotubes to that on any other hydrophobic surface supports the use in our model of the geometrical parameters known from extensive crystallographic studies.

Streptavidin is a tetrameric protein of  $M_r = 64\,000$ .<sup>23</sup> According to electrophoretic measurements, it is electrically

neutral at pH values between 6 and 7.2.<sup>24</sup> However, it contains a number of residues with strong side-chain bases.<sup>25–30</sup> Each streptavidin monomer has two histidine residues. His-87 is located close to the biotin binding pocket on the “top” and “bottom” of the protein, and His-127 residues lie on the long side of the barrel at the interface between two subunits. Histidine is one of the strongest bases at physiological pH (7.0), and it plays a major role in streptavidin’s recognition of biotin.<sup>23</sup> For other important base-containing residues such as lysine and arginine, only some of the residues have been specifically located in the tertiary structure. On the basis of those locations that have been identified, we estimate that the external envelope of the protein contains 80 arginine residues and 20 lysine residues for a total of 100 amine groups.

The effects of adsorbed amines on nanotube electronic properties have been studied by several authors.<sup>22,31,32</sup> The most quantitative measurement has shown that 0.04 electrons per adsorbed amine are donated to semiconducting nanotubes.<sup>22,31</sup> This charge donation is detected as a shift in the threshold voltage of nanotube transistors toward negative gate voltages. The observation of a shift indicates that this effect plays a role in protein adsorption as well. The magnitude of the charge transfer from proteins can be assessed by comparing our simple protein model with previous measurements using  $\text{NH}_3$ <sup>22</sup> and poly(ethylene imine) (PEI).<sup>32,33</sup>

First, the number of amine groups can be estimated using a simple model in which roughly spherical proteins cover the top half of the cylindrical nanotube. The proteins are assumed to coat the available nanotube surface with amine groups proportional to the surface area in contact. The nanotube under consideration here has a diameter of 2.4 nm (as reflected in the small band gap observed in Figure 3B) so that the surface area in contact with each 5-nm protein is  $\pi/2 \times 2.4 \times 5 \text{ nm}^2$ . Each protein surface contains 100 amine groups distributed over the 5-nm sphere so that on average each protein contacts the nanotube with 20 amine groups. Because the proteins are 5 nm in diameter, we assume that 200 proteins are adsorbed on the 1- $\mu\text{m}$  nanotube. Thus, the monolayer of adsorbed protein contacts the nanotube with 4000 adsorbed amine groups.

By comparison, commercially available PEI is a highly branched polymer with a molecular weight of about 25 000 and about 500 monomers per chain. About 25% of the amino groups of PEI are primary, with about 50% secondary and 25% tertiary. The deposition of PEI on nanotube devices results in negative shifts in the device threshold voltages, with a fully coated nanotube showing a shift of approximately  $-12 \text{ V}$ . The amount of charge transfer depends on the number of amino groups in the polymer and their basicity. This has been confirmed by the deposition of PEI polymer from different aqueous solutions with different pH values.<sup>34</sup> Computer modeling has been used to evaluate the density of amino groups in the adsorbed PEI polymer, with the conclusion that 3–10 amino groups are located on 1  $\text{nm}^2$  of polymer surface area.<sup>34</sup> Because the monomers are small and mobile in the case of the polymer, we assume that the full nanotube circumference is available for adsorption. Thus,



the 1- $\mu\text{m}$  nanotube adsorbs 23 000 to 75 000 amine groups from PEI. Approximately 10 times more amine groups adsorb from PEI than from streptavidin. This is consistent with the significantly larger threshold shift that is observed after PEI deposition.

The specific quantity of charge transferred can be estimated using the calibration provided by measurements of ammonia adsorption, which have found that each adsorbed group donates 0.04 electrons. Given the capacitance between the nanotube and the gate, the quantity of donated charge can be related to the observed threshold shift.<sup>22</sup> The capacitance depends on the nanotube diameter, and for a nanotube of diameter 2.4 nm, it is approximately 500 aF<sup>21</sup>. If the 4000 amine groups are contributed from the adsorbed proteins, with each group donating 0.04 electrons, this represents a quantity  $Q = 26$  aC of donated charge. Because the nanotube capacitance to the liquid gate,  $C$ , is 500 aF, this donated charge should produce a threshold shift, given by  $\Delta V = Q/C$ , of  $-50$  mV. By comparison, the observed threshold shift in the presence of a monolayer of protein in buffer is  $-60 \pm 3$  mV. The equivalent shift measured using the substrate gate in a dry environment, as in Figure 4, would be 1.2 V. The larger shift, 5 V, that is observed in that case is due to the additional charge transfer from the protein that is no longer surrounded by buffer.

This model accounts for the threshold shift observed in liquid using only the basic residues. Other less basic residues, particularly phenolic residues such as tryptophan and tyrosine, may also play a secondary role, since aromatic molecules are known to affect nanotube electronic properties.<sup>35,36</sup> In addition, a more detailed model of the protein–nanotube interaction is necessary to quantify more precisely how many basic residues contact the nanotube. However, as a first comparison, our simple model explains the observed threshold shift remarkably well. Two different comparisons, to PEI and to  $\text{NH}_3$ , agree, giving strong evidence that proteins donate charge to carbon nanotubes.

The charge-transfer mechanism that we have identified may have implications on a broad range of areas where immobilization is attempted and used for fundamental studies and also for applications. Such interactions also involve functional groups different from those involved in hydrophobic interactions and thus may lead to different attachment geometries in the two cases. Experiments involving a variety of proteins may shed light on the issues raised in this communication. The relatively weak interaction (in contrast to cases where immobilization is via functional groups attached to the nanotubes) that is involved also suggests that applied electric fields may have a significant influence on the immobilization. Experiments are being conducted to determine if this is indeed the case.

## References

- (1) Robers, M.; Rensink, I. J. A. M.; Hack, C. E.; Aarden, L. A.; Reutelingsperger, C. P. M.; Glatz, J. F. C.; Hermens, W. T. *Biophys. J.* **1999**, *76*, 2769–2776.
- (2) McNeil, C. J.; Athey, D.; Ho, W. O. *Biosens. Bioelectron.* **1995**, *10*, 75–83.
- (3) Turner, D. C.; Chang, C. Y.; Fang, K.; Brandow, S. L.; Murphy, D. B. *Biophys. J.* **1995**, *69*, 2782–2789.

- (4) Wadu-Mesthrige, K.; Amro, N. A.; Garno, J. C.; Xu, S.; Liu, G.-Y. *Biophys. J.* **2001**, *80*, 1891–1899.
- (5) Nicolau, D. V.; Taguchi, T.; Taniguchi, H.; Yoshikawa, S. *Langmuir* **1998**, *14*, 1927–1936.
- (6) Pompa, P. P.; Blasi, L.; Longo, L.; Cingolani, R.; Ciccarella, G.; Vasapollo, G.; Rinaldi, R.; Rizzello, A.; Storelli, C.; Maffia, M. *Phys. Rev. E* **2003**, *67*, 41902–1–8.
- (7) Sagvolden, G. *Biophys. J.* **1999**, *77*, 526–532.
- (8) Shim, M.; Kam, N. W. Shi; Chen, R. J.; Li, Y.; Dai, H. *Nano Lett.* **2002**, *2*, 285–288.
- (9) Huang, W.; Taylor, S.; Fu, K.; Lin, Y.; Zhang, D.; Hanks, T. W.; Rao, A. M.; Sun, Y.-P. *Nano Lett.* **2002**, *2*, 311–314.
- (10) Chen, R. J.; Zhang, Y.; Wang, D.; Dai, H. *J. Am. Chem. Soc.* **2001**, *123*, 3838–3839.
- (11) Davis, J. J.; Green, M. L. H.; Hill, H. A. O.; Leung, Y. C.; Sadler, P. J.; Sloan, J.; Xavier, A. V.; Tsang, S. C. *Inorg. Chim. Acta* **1998**, *272*, 261–266.
- (12) Balavoine, F.; Schultz, P.; Richard, C.; Mallouh, V.; Ebbesen, T. W.; Mioskowski, C. *Angew. Chem., Int. Ed.* **1999**, *38*, 1912–1915.
- (13) Dieckmann, G. R.; Dalton, A. B.; Johnson, P. A.; Razal, J.; Chen, J.; Giordano, G. M.; Munoz, E.; Musselman, I. H.; Baughman, R. H.; Draper, R. K. *J. Am. Chem. Soc.* **2003**, *125*, 1770–1777.
- (14) Bachtold, A.; Hadley, P.; Nakanishi, T.; Dekker, C. *Science* **2001**, *294*, 1317–1320.
- (15) Martel, R.; Schmidt, T.; Shea, H. R.; Hertel, T.; Avouris, Ph. *Appl. Phys. Lett.* **1998**, *73*, 2447–2449.
- (16) Besteman, K.; Lee, J.-O.; Wiertz, F. G. M.; Heering, H. A.; Dekker, C. *Nano Lett.* **2003**, *3*, 727–730.
- (17) Chen, R. J.; Bangsaruntip, S.; Drouvalakis, K. A.; Shi Kam, N. W.; Shim, M.; Li, Y.; Kim, W.; Utz, P. J.; Dai, H. *Proc. Natl. Acad. Sci. U.S.A.* **2003**, *100*, 4984–4989.
- (18) Star, A.; Gabriel, J.-C. P.; Bradley, K.; Grüner, G. *Nano Lett.* **2003**, *3*, 459–463.
- (19) Bradley K.; Cumings, J.; Star, A.; Gabriel, J.-C. P.; Gruner, G. *Nano Lett.* **2003**, *3*, 639–641.
- (20) Krueger, M.; Buitelaar, M. R.; Nussbaumer, T.; Schönenberger, C.; Forró, L. *Appl. Phys. Lett.* **2001**, *78*, 1291–1293.
- (21) Rosenblatt, S.; Yaish, Y.; Park, J.; Gore, J.; Sazonova, V.; McEuen, P. L. *Nano Lett.* **2002**, *2*, 869–872.
- (22) Bradley, K.; Gabriel, J.-C. P.; Briman, M.; Star, A.; Grüner, G. *Phys. Rev. Lett.* **2003**, *91*, 218301.
- (23) Weber, P. C.; Ohlendorf, D. H.; Wendoloski, J. J.; Salemme, F. R. *Science* **1989**, *243*, 85–88.
- (24) van Oss, C. J.; Giese, R. F.; Bronson, P. M.; Docoslis, A.; Edwards, P.; Ruyechan, W. T. *Colloids Surf., B* **2003**, *30*, 25–36.
- (25) Hendrickson, W. A.; Pähler, A.; Smith, J. L.; Satow, Y.; Merritt, E. A.; Phizacker, R. P. *Proc. Natl. Acad. Sci. U.S.A.* **1989**, *86*, 2190–2194.
- (26) Weber, P. C.; Wendoloski, J. J.; Pantoliano, M. W.; Salemme, F. R. *J. Am. Chem. Soc.* **1992**, *114*, 3197–3200.
- (27) Frey, W.; Schief, W. R., Jr.; Pack, D. W.; Chen, C.-T.; Chilkoti, A.; Stayton, P.; Vogel, V.; Arnold, F. A. *Proc. Natl. Acad. Sci. U.S.A.* **1996**, *93*, 4937–4941.
- (28) Athappilly, F. K.; Hendrickson, W. A. *Protein Sci.* **1997**, *6*, 1338–1342.
- (29) Yacilla, M. T.; Robertson, C. R.; Gast, A. P. *Langmuir* **1998**, *14*, 497–503.
- (30) Wang, S.-W.; Robertson, C. R.; Gast, A. P. *Langmuir* **2000**, *16*, 5199–5204.
- (31) Chang, H.; Lee, J. D.; Lee, S. M.; Lee, Y. H. *Appl. Phys. Lett.* **2001**, *79*, 3863–3865.
- (32) Kong, J.; Dai, H. *J. Phys. Chem. B* **2001**, *105*, 2890–2893.
- (33) Shim, M.; Javey, A.; Kam, N. W. S.; Dai, H. *J. Am. Chem. Soc.* **2001**, *123*, 11512–11513.
- (34) Star, A.; Han, T.-R.; Joshi, V.; Gruner, G. *Polym. Prep.* **2003**, *44*, 201.
- (35) Sumanasekera G. U.; Pradhan, B. K.; Romero, H. E.; Adu, K. W.; Eklund, P. C. *Phys. Rev. Lett.* **2002**, *89*, 166801.
- (36) Star, A.; Han, T.-R.; Gabriel, J.-C. P.; Bradley, K.; Grüner, G. *Nano Lett.* **2003**, *3*, 1421–1423.

NL0349855